

Design, modeling and control of a soft gripper with TCP actuator using image processing

1- Hamidreza Arefi
department of mechatronics
engineering University of Tabriz
Tabriz, iran
hamidray76@gmail.com

2- Behnam Dadashzadeh
department of mechatronics
engineering University of Tabriz
Tabriz, iran
b.dadashzadeh@tabrizu.ac.ir

3- Akbar Allahverdizadeh
department of mechatronics
engineering University of Tabriz
Tabriz, iran
allahverdizadeh@tabrizu.ac.ir

4- Reza Abdollahi
department of mechatronics
engineering University of Tabriz
Tabriz, iran
r.abdollahi98@ms.tabrizu.ac.ir

Abstract— Artificial muscles have gained importance due to their high deformability, which is used in soft robots. In this article, to further exploit and understand the behavior of TCP muscles, as well as to control these muscles more easily, we mathematically model the stimulus, which includes a model to understand the temperature behavior of muscles with changes in flow and amount of displacement due to changes in temperature and amount of external force. is. By designing a soft gripper and applying the necessary restrictions, we get the force needed to move this gripper. Then we obtain the kinematic model of the finger to obtain the bending angle due to the displacement of the muscle which is connected to the fingers and gripper by the cable. We also check the muscle's ability to perform this movement. In the next step, programming and implementation of a simple model of turning on and off the heating and cooling system to create expansion and contraction in the muscle is done by image processing on the Arduino controller to control the system. Using the obtained models and taking into account different and important values in the models, we extracted the related diagrams and checked and compared them. From these results, we can point out the changes in the temperature behavior and movement of the muscle with the change in the input current as well as the type of alloy used, the controllability of the muscle, and the ability of the muscle to move the gripper.

Keywords— Polymer muscle - artificial muscle - robotics - soft robot - soft gripper - TCP actuator - machine vision - image processing

I. INTRODUCTION

A: Soft Robot

Traditional robots have rigid structures that limit their ability to interact with their environment. These robots often work in unstructured and crowded environments. To improve this problem, researchers have started designing and building soft robots inspired by nature [1] Animals can move in complex environments due to the flexible structure of their bodies. These capabilities have motivated robotics engineers to incorporate soft technologies into their designs [2] Advances in the field of soft robots will depend on advances in materials

science. The use of fluids, elastomers, gels and other soft materials are challenged in this field [3] While rigid robots are made of hard materials such as metals and hard plastics, soft robots must be made of soft materials or a strategic combination of materials. be made soft and hard with maximum elasticity [4]

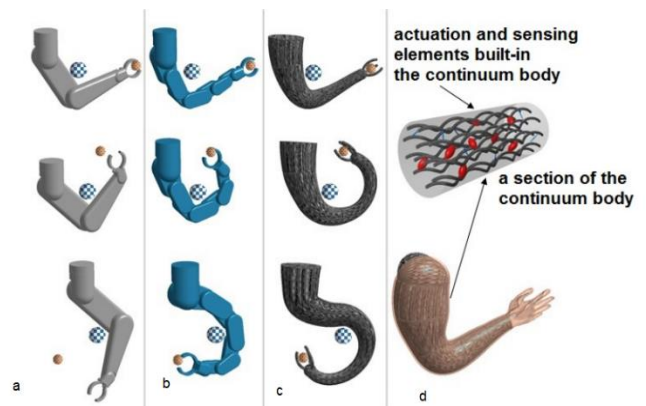


Figure 1: Comparison between: a) a conventional robot hand b) an overmatched robot hand c) a soft robot hand d) a soft robotic arm with a continuous topology that integrates actuator and sensor elements in the same continuous body. [5]

Compared to rigid robots, soft robots have problems in modeling, calibration and control, because the inherent characteristics of soft materials can create complex behaviors due to nonlinearity [6].

B: TCP driver

With advantages such as low cost and light weight, thermal actuators are suitable for use in robotics and biomechanics. Using these operators for practical applications requires understanding their behavior in response to electrical input [7].

Twisted and helical polymers (TCP) can generate large motions and generate high power density, which makes them a promising artificial muscle. One of the applications that

have been noticed for TCP actuators in recent years due to their reasonable price and at the same time high efficiency is the use of these actuators in robot fingers [8]. Twisted and helical polymers (TCP) can generate large motions and generate high power densities, making them a promising artificial muscle.

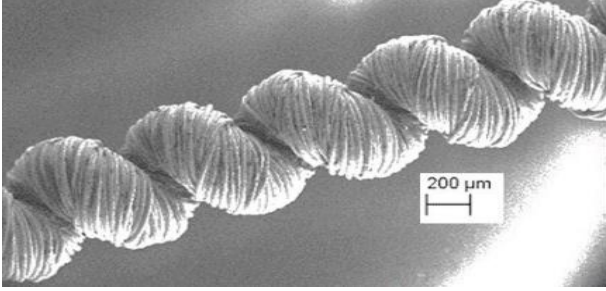


Figure 2: Microscopic view of a TCP muscle [9]

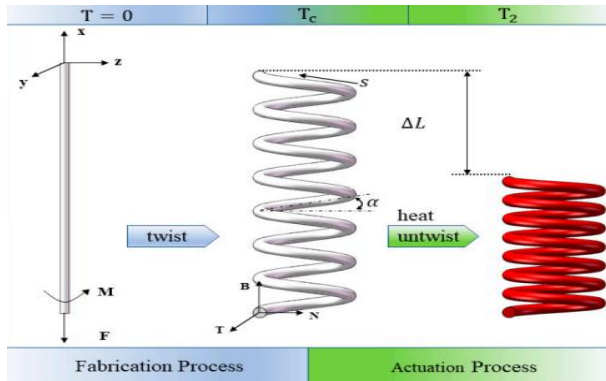


Figure 3: Schematic of the heat-induced stretch stimulation process in twisted and untwisted polymer muscle [10]

II. MATHEMATICAL MODELING OF TCP DRIVE

The geometry of TCP muscles is like a long string that has size in one dimension. Knowing that the heat flux starts from the fibers that are located along the length of the muscle and considering the same resistance, it can be said that the heat flux mainly flows from the conductive fibers towards the surface of the muscle, which is negligible in the length direction.

Considering the length of the TCP muscle [11] as the control volume, the heat transfer with the surrounding environment will be the boundary condition, also there is heat generation by Joule heating inside the control volume. Using the first law of thermodynamics for the defined control volume, we have:

$$mc_p \frac{dT}{dt} = -hA(T - T_\infty) + i^2R \quad (1)$$

where m is the mass, c_p is the specific heat capacity, h is the displacement heat transfer coefficient, A is the area exposed to the ambient air, i is the driving current, and R is the electrical resistance of the TCP muscle. We can define the resistance of conductors as follows:

$$R = \rho \frac{L}{A} \quad (2)$$

where ρ is the specific resistance, L is the length and A is the area of the conductive part. On the other hand, the specific resistance of metals is sensitive to temperature changes. For

metals such as what is inside the TCP muscle these changes are shown as follows:

$$\rho(T) = \rho_0(1 + \alpha(T - T_0)) \quad (3)$$

where ρ_0 is the resistance at the reference temperature, α is the temperature resistance coefficient, and T_0 is the initial temperature. Now, according to relation (2) and assuming the same geometry and placing it in relation (3), we have:

$$R(T) = R_0(1 + \alpha(T - T_0)) \quad (4)$$

Now, by inserting the obtained equation in the equation (1) and assuming $T_0 = T_\infty$, the final equation is obtained as follows:

$$mc_p \frac{d(T - T_\infty)}{dt} = (-hA + i^2R_0\alpha)(T - T_\infty) + i^2R_0 \quad (5)$$

The result obtained by using the above equation is that if the value of $i^2R_0\alpha$ becomes greater than hA , the above differential equation will become unstable and as a result the temperature will increase. The solution of the above equation for the initial temperature equal to the ambient temperature and the amount of time equal to zero for the state of muscle contraction is as follows:

$$T - T_\infty = \frac{R_0 i^2}{-hA + R_0 i^2 \alpha} \left(1 - e^{\frac{-hA + R_0 i^2 \alpha}{mc_p} t} \right) \quad (6)$$

Also, by setting time equal to 140, muscle temperature equal to 70 degrees Celsius and flow equal to zero, for equation (5) and muscle expansion state, we will have:

$$T - T_\infty = 44e^{\frac{hA}{mc_p}(140-t)} \quad (7)$$

To obtain a model for muscle displacement, we must consider two components, one of which is the stretch caused by the load in the muscle and the second is the contraction caused by heat. First, we go to the displacement due to stretching by load and external force Δ_{el} .

$$\Delta_{el} = F/k \quad (8)$$

where F is the external load in the muscle and k is the stiffness of the muscle obtained by the laboratory results. In the following, we use the geometry of the muscle shown in the figure below to find the change in muscle length.

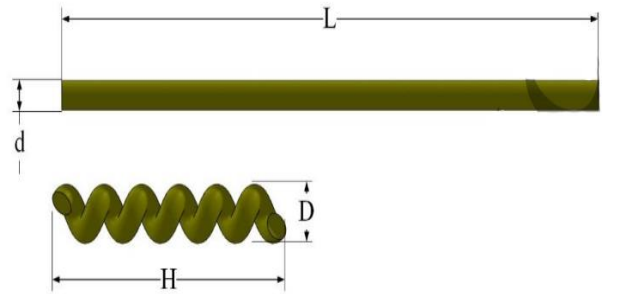


Figure 4: Geometrical parameters of TCP muscle

The length of the muscle can be considered as follows:

$$H = \sqrt{L^2 - \pi D^2} \quad (9)$$

where H is the length of the muscle, D is the diameter of the muscle, and L is the length of the precursor muscle. By deriving from the above relation assuming linearity of thermal expansion coefficient, we will have:

$$\begin{aligned} \Delta_{th} = \delta H &= \frac{L\delta L}{\sqrt{L^2 - \pi D^2}} - \frac{\pi D\delta D}{\sqrt{L^2 - \pi D^2}} \\ &= \frac{L^2}{H} a_1 (T - T_0) - \frac{\pi D^2}{H} a_2 (T - T_0) \end{aligned} \quad (10)$$

where a is the coefficient of thermal expansion in both longitudinal and radial directions. Now, considering these two components, assuming the geometry does not change during stimulation, the displacement of the whole muscle Δ_H can be obtained as follows:

$$\Delta_H = H - \Delta_{th} + \Delta_{el} \quad (11)$$

where Δ_{th} is the thermal displacement and Δ_{el} is the displacement caused by tension. Finally, by placing the relevant relationships in equation (11), the final model is obtained as follows:

$$\Delta_H = H - \left(\frac{L^2}{H} - \frac{\pi D^2}{H} \right) (c_1 T + c_2) (T - T_0) + F/k \quad (12)$$

III. SOFT GRIPPER DESIGN AND SOFT FINGER CONSTRUCTION

A. Soft gripper design

We have designed a soft silicone gripper consisting of three fingers. In general, the body of a suitable soft finger should have the following characteristics:

- 1- It should be soft and flexible enough and have little resistance to bending and opening.
- 2- It should be small and compact so that it can show the same function as a human finger.

One of the obstacles that made it difficult for us to design a soft gripper was the lack of a design and simulation environment for soft robots. For this reason, we used ADAMS software. In order for the robot's finger to be similar to a human finger, we used two hinges in its design, which are reminiscent of the two middle fingers in each human finger. We chose the dimensions of the finger with a length of 14.5 cm, width and height of 2 cm. By drawing one finger and extending it to the other two fingers, we fix them at an angle of 120 degrees apart on a fixed page to get the general view of the gripper.

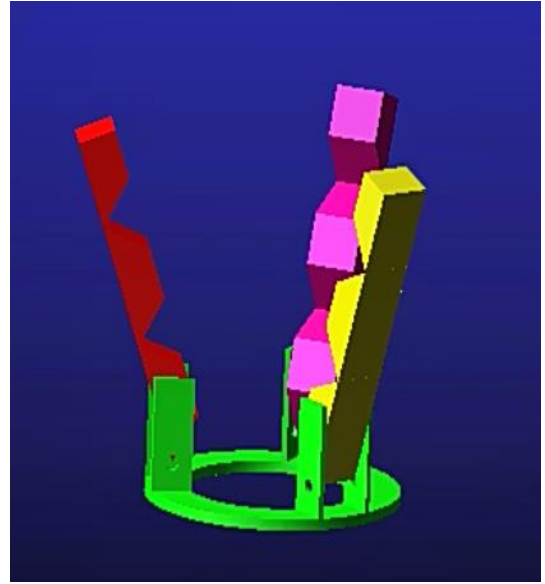


Figure 5: Schematic of the final soft gripper

After designing the gripper, the next step is to design the movement mechanism for the gripper. To connect the fingers to the actuator, we use cables that pass through each finger and finally connect to the actuator with a fixed end, and to return the finger to its original state, we also use the Fenrite constant on the back of each finger. Since we did not have the possibility to design the cables inside the finger in the software environment, we applied its movement and effect using annotations.

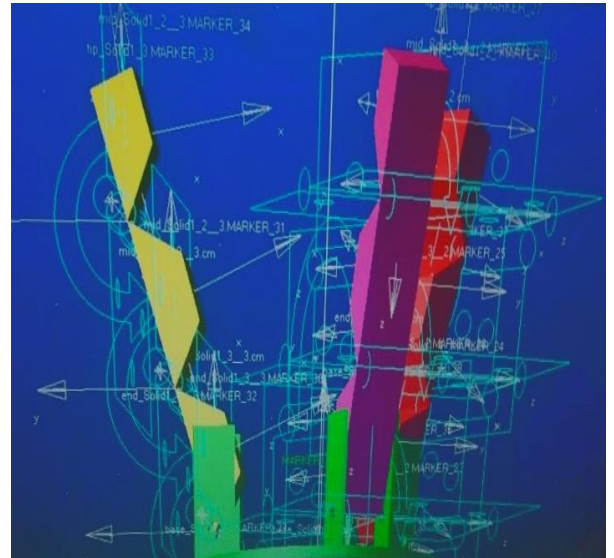


Figure 6: Gripper stipulations method

Next, we show the kinematics of the finger. By considering the fixed radius of curvature, we can get the bending angle of the finger. According to the figure below, which is a representation of the finger in a bent state, where l is the length of the finger, l_t is the length of the tendon, θ is the bending angle, r is the radius of curvature, and d is the distance of the tendon from the cross section of the finger:

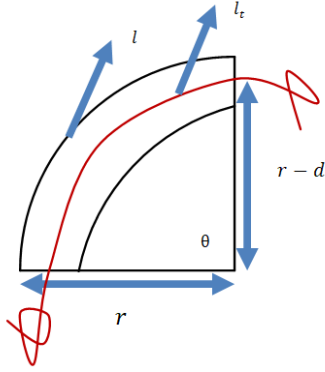


Figure 7: Finger kinematics

$$l = r\theta \quad (13)$$

$$l_t = (r - d)\theta \quad (14)$$

$$\Delta l = l - l_t = \theta d \quad (15)$$

Finally, for the bending angle we will have:

$$\theta = \Delta l / d \quad (16)$$

B. Gripper opening and closing control using machine vision

In this step, we will discuss how to write code to control the opening and closing of the voltage with the help of machine vision and Python software. In the system under our study, the TCP actuator is compressed and expanded by the heating and cooling system, which can be done by reaching the current to the two mentioned systems. What was done at this stage was that the camera, by detecting the hand in a fully open position, sends the current to the heating system, and by detecting the hand in a fully closed fist position, the camera sends the current to the cooling system, which is responsible for muscle contraction. At first, we go to programming for identification.

For this purpose, we use two libraries in Python named opencv and Mediapipe. These two libraries are image processing and machine vision libraries. Mediapipe uses machine learning to detect hand position and uses RGB video frames to detect hand key points. This library uses a two-step identifier to identify the hand's condition, which first finds the location and placement of the specified part inside the frame, and in the next step predicts the number of key points for the hand, which is 21.

To estimate the position and posture of the hand, we must first model it, which includes extracting the position of hand components such as fingers and palm and placing them on the hand. One of Mediapipe's solutions, in addition to face recognition and segmentation, is determining the hand model, and for this, it uses a convolutional neural network. Finally, a hand model characterized by 21 landmarks is obtained. [12]

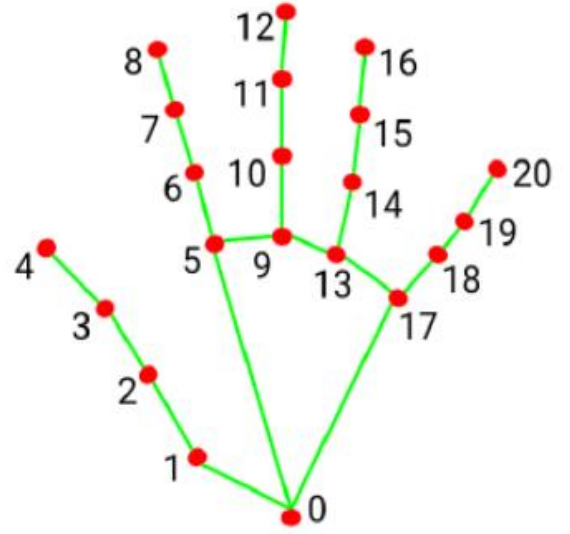


Figure 8: Hand model with 21 milestones [12]

For our purpose, which was to identify the hand in two ways, open and closed, an open hand is defined when all 5 fingers are fully open, and a closed hand is defined when all 5 fingers are fully closed. Identification of open and closed hands is shown as 5 fingers are open and none of the fingers are open as below.

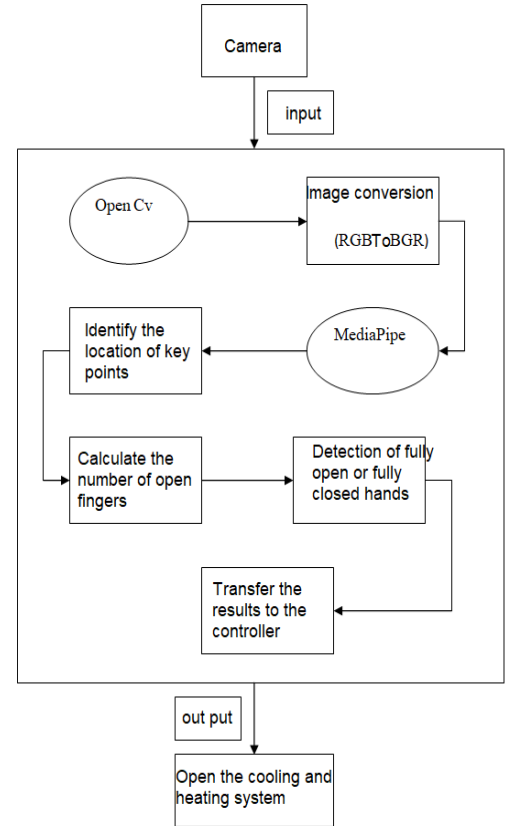


Figure 9: Flowchart of hand recognition

Finally, the identification of open and closed hands is shown in the form of 5 fingers being open and none of the fingers being open.



Figure 10: Open hand detection

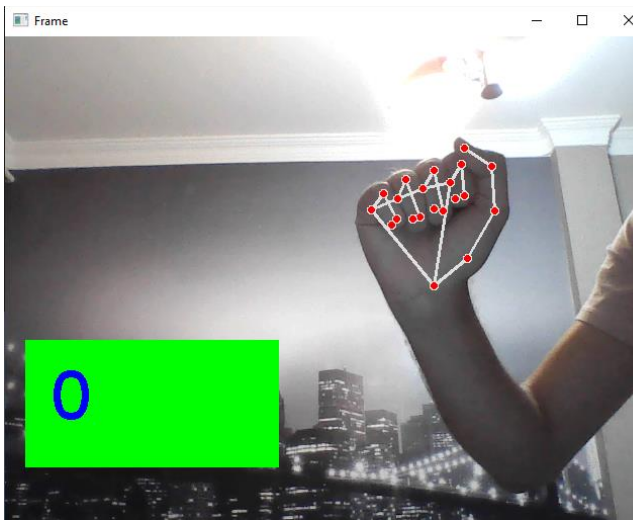


Figure 11: Closed hands detection

We took the help of Arduino to show the flow of current to the two systems in question. In this way, two heating and cooling systems were simulated with two LED lights, and they turned on and off by receiving the hand command to open and close.

We used the Pyfirmata library to connect the Arduino board and Python, and after defining the desired function, we added it to the main program and transferred it to the Arduino board.

IV. RESULTS AND DISCUSSION

By examining the relationships obtained in connection with mathematical modeling and solving the equations obtained from it, we can obtain the temperature changes over time in two states of contraction and expansion or heating and cooling. For this, according to the different initial conditions and putting the relevant values in the equations with the help of MATLAB software, we obtain three outputs for each of the heating and cooling modes for three different input streams.

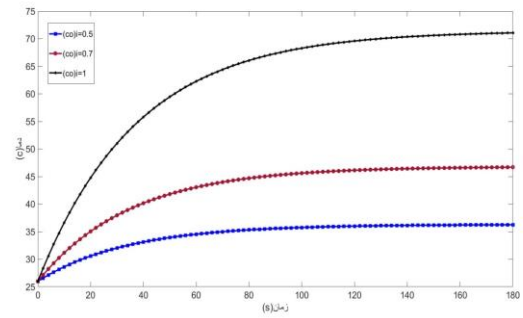


Figure 12: Modeling output in the muscle contraction phase for three currents of 0.5, 0.7, and 1 amps.

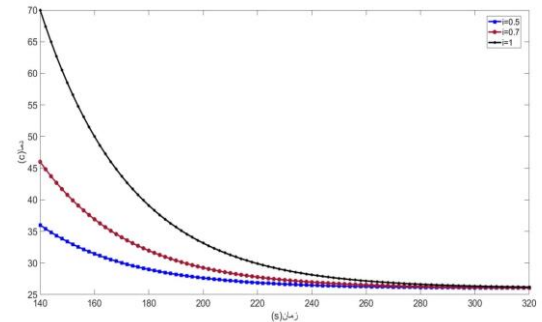


Figure 13: Modeling output in the muscle expansion phase for three currents of 0.5, 0.7, and 1 amps.

By examining the above, we can conclude that the muscle in different streams reaches a constant temperature after a period of time that is different for each stream. Also, as shown in the diagram, we can increase the contraction speed by using higher power. By further examining the two graphs, it can be seen that approximately equal time is required for both contraction and expansion cycles.

In the results obtained from these studies, from a nickel-titanium alloy that is irradiated like a spring and has a diameter of about 0.2 mm with a constant voltage of about 8 volts, we can see the following diagram.

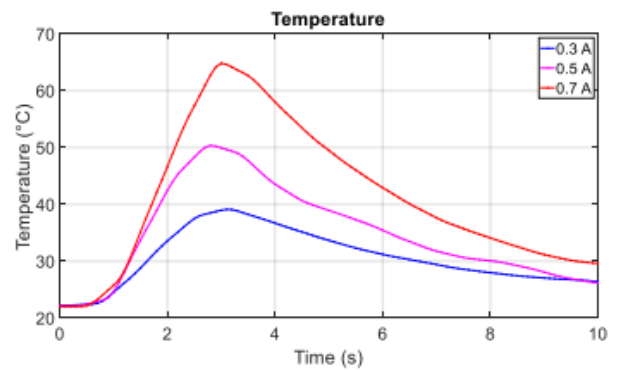


Figure 14: Output of SMA muscle temperature changes

By checking the diagram above and the approximate current of 0.7 amps, which produces a temperature of about 70 degrees Celsius and needs about 3 seconds for this. Also, in the return and cooling cycle, we observe a time of about 7 seconds during which the actuator returns to its initial state. By checking the diagram, we needed a current of 1 amp in about 140 seconds to reach a temperature of 70 degrees Celsius, which indicates a more acceptable performance for

the SMA muscle in almost the same conditions. Also, the time required for the cooling cycle for the SMA muscle is much longer than the heating cycle, and this issue makes the controllability of the muscle difficult. In the following, according to the modeling developed for muscle movement such as temperature changes, the graph of the state of expansion and contraction is obtained as follows:

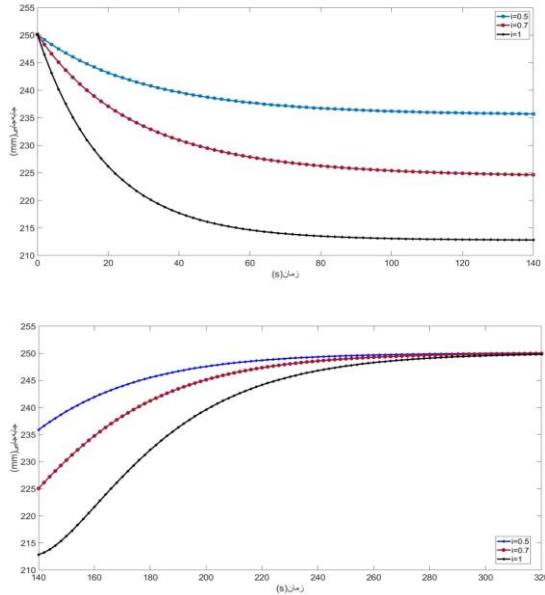


Figure 15: Muscle displacement in two states of contraction and expansion

According to the diagram, it can be said that displacement increases with increasing current, and for higher currents, displacement of the muscle will be more promising. On the other hand, increasing the current should not cause the loss of our precursor fiber, so this issue is known as a fundamental limitation for working with TCP drivers. Since the bending angle of the finger has a direct relationship with the amount of displacement, so the above problem will be undeniable for more bending of the finger. Regarding the value of the bending angle, according to the graphs obtained, it can be concluded that with the increase in the current, the bending value of the finger connected to the actuator will increase.

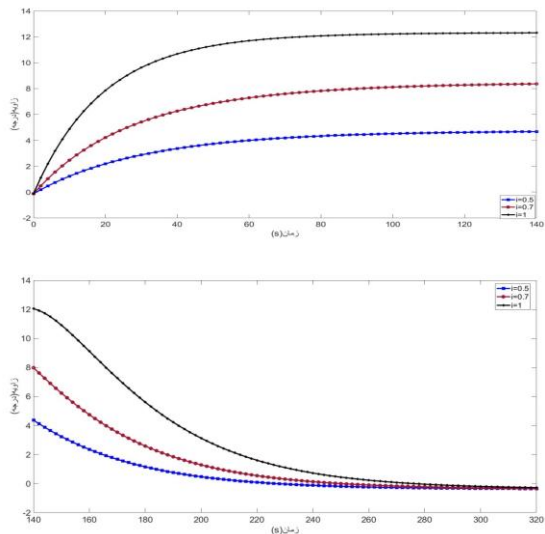


Figure 16: Finger bending angle in two states of muscle contraction and expansion

For low currents of one amp, this amount of bending angle is very small. By changing the material of the coil from copper to nickel chrome due to the higher specific resistance and also the specific heat capacity in nickel chrome metal, we can compare the temperature behavior of two different types of coil.

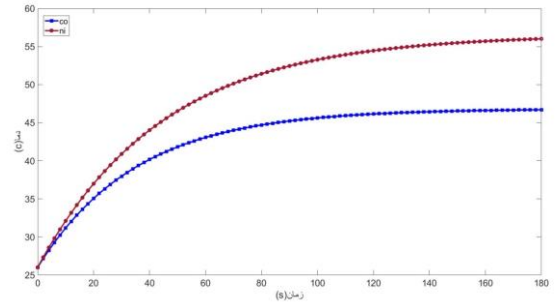


Figure 17: Temperature comparison of the muscle in the state of contraction with two copper and nickel chrome coils

According to the above diagram, we find that the muscle shows higher temperature changes with nickel-chromium metal than with copper. Also, these changes will be valid for displacement and bending angles.

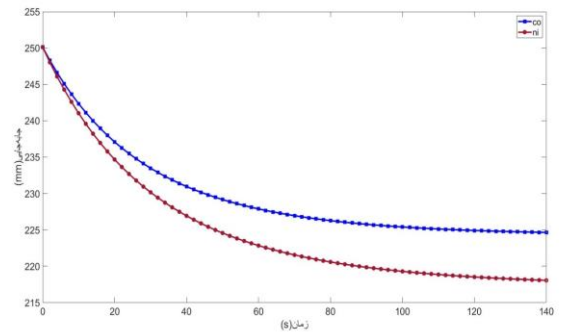


Figure 18: Comparison of muscle displacement in the state of contraction with two copper and nickel chrome coils

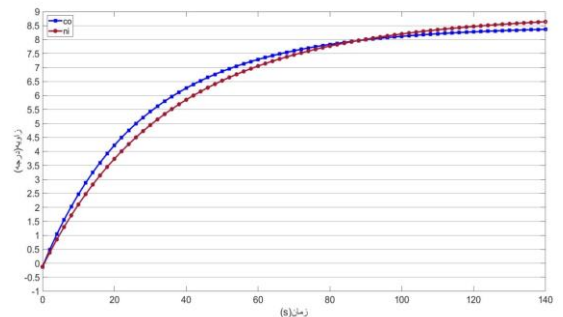


Figure 19: Comparison of the bending angle in the state of muscle contraction with two coils of copper and nickel-chromium

After performing dynamic analysis on the simulated gripper in the ADAMS environment and referring to the muscle power according to reference [13], we investigate the ability of the muscle to move the gripper. By further examining the experimental work done on the TCP driver, the following results are obtained:

Table 1: Laboratory results from reference [13]

type of muscle	Amount of weight (grams)	base voltage (V)	Percentage of muscle displacement
1 ply	60	0.98	12.5
1 ply	60	1.37	16.6
1 ply	280	0.98	15
1 ply	280	1.37	28
2 ply	280	1.37	12.9

With the design of the gripper and the application of high forces, which included the forces of 0.6 and 2.8 newtons, we saw the movement of the gripper. By examining the gripper model, we concluded that the minimum force required to reach three fingers to one another is 10 newtons. Therefore, by increasing the number of muscles, we must supply this force.

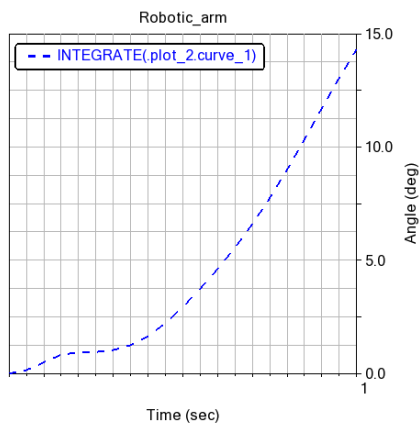


Figure 20: Bending-time diagram of gripper

Finally, by closing the Arduino controller and transferring the program, the result was obtained correctly

REFERENCES

- [1] Trivedi, D., Rahn, C. D., Kier, W. M., & Walker, I. D. (2008). Soft robotics: Biological inspiration, state of the art, and future research. *Applied bionics and biomechanics*, 5(3), 99-117.
- [2] Kim, S., Laschi, C., & Trimmer, B. (2013). Soft robotics: a bioinspired evolution in robotics. *Trends in biotechnology*, 31(5), 287-294.
- [3] Majidi, C. (2019). *Soft-matter engineering for soft robotics*. *Advanced Materials Technologies*, 4(2), 1800477.
- [4] Alici, G. (2018). Softer is harder: What differentiates soft robotics from hard robotics?. *MRS Advances*, 3(28), 1557-1568.
- [5] Mazzolai, B., Mondini, A., Del Dotore, E., Margheri, L., Carpi, F., Suzumori, K., ... & Lendlein, A. (2022). Roadmap on soft robotics: multifunctionality, adaptability and growth without borders. *Multifunctional Materials*, 5(3), 032001.
- [6] Kim, D., Kim, S. H., Kim, T., Kang, B. B., Lee, M., Park, W., ... & Jo, S. (2021). Review of machine learning methods in soft robotics. *Plos one*, 16(2), e0246102.
- [7] Karami, F., Wu, L., & Tadesse, Y. (2020). Modeling of one-ply and two-ply twisted and coiled polymer artificial muscles. *IEEE/ASME Transactions on Mechatronics*, 26(1), 300-310.
- [8] Wu, C., & Zheng, W. (2020, April). A modeling of twisted and coiled polymer artificial muscles based on elastic rod theory. In *Actuators* (Vol. 9, No. 2, p. 25). MDPI.
- [9] AlmuBarak, Y., & Tadesse, Y. (2017). Twisted and coiled polymer (TCP) muscles embedded in silicone elastomer for use in soft robot. *International Journal of Intelligent Robotics and Applications*, 1, 352-368.
- [10] Kar, D., George, B., & Sridharan, K. (2022). A review on flexible sensors for soft robotics. *Systems for Printed Flexible Sensors: Design and implementation*, 1-1.
- [11] Karami, F., & Tadesse, Y. (2017, November). Modeling of TCP muscles for understanding actuation behavior. In *ASME International Mechanical Engineering Congress and Exposition* (Vol. 58370, p. V04AT05A060). American Society of Mechanical Engineers.
- [12] Vakunov, A., Chang, C. L., Zhang, F., Sung, G., Grundmann, M., & Bazarevsky, V. (2020). Mediapipe hands: On-device real-time hand tracking.
- [13] . خانم‌شناس، ف، (۱۴۰۰) طراحی، ساخت و کنترل یک عضله مصنوعی TCP، کارشناسی ارشد، دانشکده مکانیک، دانشگاه تبریز، ایران

IEEE conference templates contain guidance text for composing and formatting conference papers. Please ensure that all template text is removed from your conference paper prior to submission to the conference. Failure to remove template text from your paper may result in your paper not being published.